ARTICLE

Low-temperature Catalytic Reduction of Nitrogen Monoxide with Carbon Monoxide on Copper Iron and Copper Cobalt Composite Oxides

Jun-sheng Shu[a], Wen-shui Xia[a*], You-jin Zhang[b], Tao Cheng[b], Min-rui Gao[b]

a. School of Food Science and Technology, Southern Yantze University, Wuxi 214122, China
b. Department of Chemistry, University of Science and Technology of China, Hefei 230026, China

(Dated: Received on January 25, 2008; Accepted on April 23, 2008)

Copper iron composite oxides (CuO/Fe_2O_3) and copper cobalt composite oxides (CuO/Co_3O_4) for the catalytic reduction of NO with CO at low temperature were prepared by co-precipitation. The catalytic activity and thermal stability of the catalysts were evaluated by a microreactor-GC system. The 100% conversion temperatures of NO are 80 °C for CuO/Fe_2O_3 and 90 °C for CuO/Co_3O_4. The catalysts possess high catalytic activity and favorable thermal stability for NO reduction with CO in a wide temperature range and long time range. A systematic study of the molar ratios of the reactants, the volume of NaOH, aging time, and calcination temperature/time was carried out to investigate the influence preparation conditions on the catalytic activity of the catalysts.

Key words: CuO/Fe_2O_3, CuO/Co_3O_4, NO reduction, Catalytic activity, Thermal stability

I. INTRODUCTION

In recent decades, the emission of various nitrogen oxides (NO_x) into the atmosphere has been occurring on a massive scale. To comply with the environmental emission standard, removal of these contaminants is necessary. The purification of these exhaust gases is regarded as one of the main goals of air pollution control [1-4].

To convert highly toxic NO into non-toxic N_2 by catalytic reaction is the most effective method of removing NO. Up to now, some success has been met in the catalytic reduction of NO. In the catalytic reduction of NO, ammonia (NH_3) [5-8], carbon monoxide (CO) [9-11], hydrocarbons [12-15], methane (CH_4) [16-20], or hydrogen (H_2) [21,22] are used as reducing agent, and noble metals [23-25], metal oxides [26,27], mesostructured alumino-silicates [28,29], pillared clays [30], active carbon [31], or perovskite-type oxides [32,33] are used as catalysts.

There are three types of catalysts for NO_x catalytic reduction [34]. Low temperature catalysts (Pt-based) were first considered for the catalytic reduction of NO_x. They are active in the catalytic reduction of NO_x at low temperature, but the selectivity and activity are poor at high temperature. The active temperature range of Pt type catalysts is 260-300 °C with 100% conversion of NO_x. When the temperature is lower than 150 °C, the catalysts are non-active on NO_x catalytic reduction [35]. The second type of catalyst is medium temperature catalysts (metal oxides). Among metal oxide mixtures, vanadia titania composite oxide (V_2O_5/TiO_2) is commonly used. In this catalyst system, the active temperature range is 320-360 °C with 100% conversion of NO_x. When the temperature is lower than 260 °C, the catalysts are non-active in NO_x catalytic reduction [36]. New Fe_2O_3 based materials have been developed for the selective catalytic reduction (SCR) of NO_x by NH_3 in diesel exhaust [6]. The highest catalytic activity is observed for ZrO_2 that is coated with 1.4 mol%Fe_2O_3 and 7.0 mol%WO_3 (1.4Fe/7.0W/Zr). By the use of this catalyst, quantitative conversion of NO_x is obtained. The third type of catalysts is high temperature catalysts (zeolite), with an active temperature range from 345 °C to 590 °C. Zeolite based catalysts present high activity only at high temperatures, and deactivate at low temperature [35].

The reaction of NO with CO is one of the most important reactions in automobile exhaust gas catalysis, in which the most used noble metals are rhodium, platinum, and palladium [37]. However, noble metals have their own problems, such as high cost, narrow active temperature range and complex pre-treatment, so we need to search for the substitutes. Consequently, considerable attention has been paid to transition metals as active component in three-way catalysts (TWCs) and automobile exhaust gas catalysts.

Nano-scale transition metals and their oxides may provide significantly improved catalytic activities over non-nano catalysts due to their small particle size, high specific surface area, more activity sites and excellent redox properties. Recently, considerable attention is given to catalytic systems with a synergistic effect. Due to the synergistic effect, the composite oxides of transition metals exhibited obviously higher catalytic activity on NO catalytic reduction [38].

This paper reports the preparation of copper iron

*Author to whom correspondence should be addressed. E-mail: zyj@ustc.edu.cn, Tel.: +86-510-85869455, Fax: +86-510-85877423

composite oxides (CuO/Fe_2O_3) and copper cobalt composite oxides (CuO/Co_3O_4) and their application in the catalytic reduction of NO with CO. To investigate the influence of preparation conditions on the catalytic activity and thermal stability, a systematic study of the preparation conditions was carried out. The results indicate that the prepared CuO/Fe_2O_3 and CuO/Co_3O_4 exhibited obviously high catalytic activity and thermal stability in a wide temperature range and long time range on NO reduction with CO. Their total conversion temperatures are 80 and 90 °C, respectively.

II. EXPERIMENTS

All chemicals, obtained from Shanghai Chemical Reagent Ltd. Co. of China, were analytical grade and used without further purification.

A. Preparation

CuO/Fe_2O_3 was prepared by co-precipitation. In a typical procedure, the aqueous solutions of 0.25 mol/L $Cu(NO_3)_2{\cdot}3H_2O$ and 0.25 mol/L $Fe(NO_3)_3{\cdot}9H_2O$ were pre-mixed in a 1:5 ratio. An aqueous solution of NaOH (25%) was added to the pre-mixed solutions under vigorous stirring at ambient temperature. The precipitates were aged in the mother liquid for several hours. Then, the precipitates were filtered, washed several times with hot, deionized water, and dried in vacuum at 80 °C for 6 h. Subsequently, the samples were calcined at different temperatures for several hours in air. The catalysts with different catalytic activities were obtained by varying the preparation conditions in the above preparation method.

The preparation process of CuO/Co_3O_4 was similar to that of CuO/Fe_2O_3, except that the premixed solution was obtained from aqueous solutions of $CuSO_4{\cdot}5H_2O$ (0.5 mol/L, 3 mL) and $CoCl_2{\cdot}6H_2O$ (0.5 mol/L, 15 mL).

B. Sample characterization

The phase purity and structure parameters of catalysts were examined by X-ray powder diffraction (XRD), using a Rigaku Dmax γ-A X-ray diffractometer with graphite-monochromatized Cu Kα radiation (λ=0.15418 nm), with a scanning rate of 0.05 °/s in the 2θ range from 10° to 70° and the operation voltage and current maintained at 40 kV and 40 mA, respectively. The transmission electron microscopy (TEM) images were recorded on a Hitachi Model H-800 instrument with a tungsten filament, using an accelerating voltage of 200 kV. The X-ray photoelectron spectral (XPS) measurements were carried out on an ESCALAB MK II X-ray photoelectron spectrometer, using Mg Kα radiation as the excitation source. The XPS spectra were corrected by adjusting the C1s peak to a position of 284.6 eV. The thermogravimetry-differential thermal analysis (TG-DTA) of the catalysts were conducted on a Rigaku Standard Model thermal analyzer (in air atmosphere, flow rate: 90 mL/min; heat rate: 10 °C/min). The specific surface areas (S_{BET}) of the catalysts were calculated from a multipoint Braunauer-Emmett-Teller (BET) analysis of the nitrogen adsorption isotherms at 77 K recorded on an Omnisorp 100CX instrument. The catalytic activity and stability of the catalysts were evaluated on a small fixed-bed microreactor operating under atmospheric pressure and an online GC using 100 mg sample of 0.18-0.45 mm. The flow rate of the feed gas was 30 mL/min. The effluent gas was analyzed with an online FuLi9790 model gas chromatograph with a Molecular Sieve 13 X column and a thermal conductivity detector (TCD). The catalysts were directly exposed to reaction gas containing (volume ratio) 1.0%NO, 5%CO, and 94.0%Ar.

III. RESULTS AND DISCUSSION

A. Structure characterization

The XRD patterns of CuO/Fe_2O_3 and CuO/Co_3O_4 calcined at different temperature are shown in Fig.1.

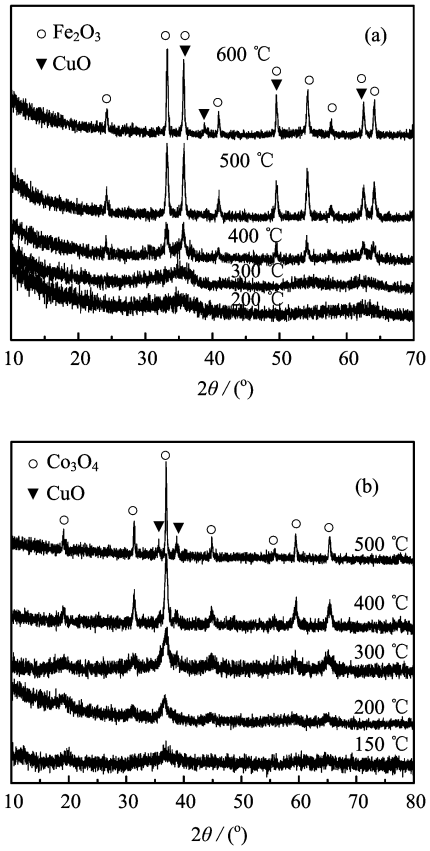

FIG. 1 XRD patterns of the catalysts. (a) CuO/Fe_2O_3. (b) CuO/Co_3O_4.

DOI:10.1088/1674-0068/21/04/393-400

From Fig.1(a), the crystallinity of CuO/Fe_2O_3 improves when the calcination temperature increases from 300 °C to 600 °C. Copper oxide and iron oxide in the CuO/Fe_2O_3 are indexed to monoclinic CuO (JCPDS No.47-937$^+$) and hexagonal Fe_2O_3 (JCPDS No.89-2810). Similarly, Figure 1(b) shows that the CuO/Co_3O_4 was amorphous when the calcination temperature was below 200 °C, but the oxides become more crystalline when the calcination temperature increases to 500 °C. Copper oxide and cobalt oxide in the CuO/Co_3O_4 are indexed to monoclinic CuO (JCPDS No.47-937$^+$) and cubic Co_3O_4 (JCPDS No.78-1970).

The XPS of the prepared CuO/Fe_2O_3 calcined at 300 °C and CuO/Co_3O_4 calcined at 200 °C are shown in Fig.2 and Fig.3. The Cu2p and Fe2p binding energies in the CuO/Fe_2O_3 are shown in Fig.2. In Fig.2(a), the peaks of $Cu2p_{3/2}$ and $Cu2p_{1/2}$ are centered at 932.5 and 952.3 eV. This suggests the presence of CuO in the CuO/Fe_2O_3 catalyst. The binding energies of $Fe2p_{3/2}$ and $Fe2p_{1/2}$ are about 710.8 and 723.8 eV (Fig.2(b)). This suggests the presence of Fe_2O_3 in the CuO/Fe_2O_3 catalyst. The Cu2p and Co2p binding energies in the CuO/Co_3O_4 catalyst are shown in Fig.3. In Fig.3(a), the peaks of $Cu2p_{3/2}$ and $Cu2p_{1/2}$ are centered at 933.8 and 953.5 eV. This suggests the presence of CuO in the CuO/Co_3O_4 catalyst. The binding energies of $Co2p_{3/2}$ and $Co2p_{1/2}$ are about 779.2 and 794.3 eV, respectively (Fig.3(b)). This suggests the presence of Co_3O_4 in the CuO/Co_3O_4 catalyst.

The general morphologies and microstructure of the catalysts were investigated by TEM and are presented in Fig.4. Figure 4(a) shows that uniform CuO/Fe_2O_3 nanoparticles were obtained with a narrow distribution. The average nanoparticle size was approximately 20 nm. From Fig.4(b), it can be seen that the CuO/Co_3O_4 nanoplates are largely formed, which may result in large S_{BET} of the catalyst.

Figure 5 depicts the typical TG-DTA curves of the CuO/Fe_2O_3 and CuO/Co_3O_4 obtained at optimal preparation conditions. In Fig.5(a), the sharp endothermic peak below 100 °C could be attributed to the loss of surface absorbed water, which is confirmed by a dramatic weight loss with 4wt% in the TG curve over the corresponding temperature range. The 7wt% weight loss from 100 °C to 500 °C on the TG curve could result from the removal of residual hydroxyl groups and crystallization process in this region. Correspondingly, no obvious endothermic peaks appeared on the DTA curve. The exothermic peaks at 540 and 610 °C on the DTA curve can be attributed to the phase transformation from γ-Fe_2O_3 to α-Fe_2O_3 and the form of copper ferrite [39]. Correspondingly, the TG curve does not show any noticeable mass loss. In Fig.5(b), the sharp endothermic peak below 100 °C could be attributed to the loss of surface absorbed water, which is confirmed by a dramatic weight loss with 3% in the TG curve over

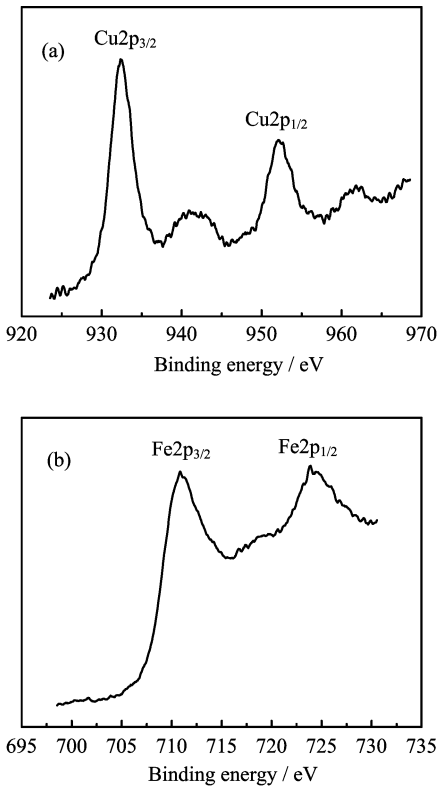

FIG. 2 XPS analysis of the copper iron catalyst calcined at 300 °C.

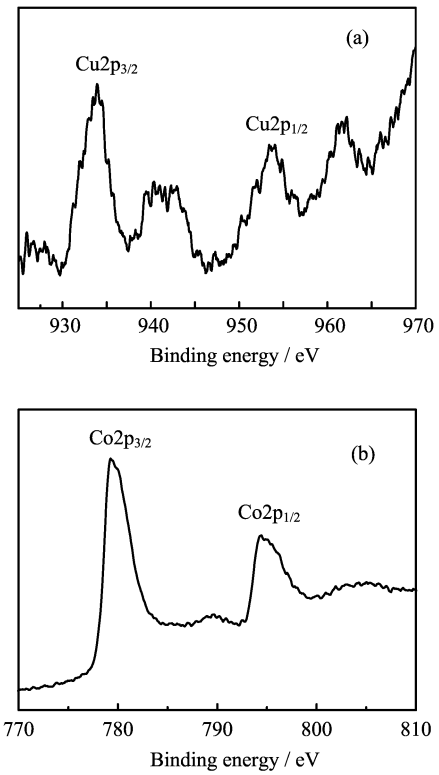

FIG. 3 XPS analysis of the copper cobalt catalyst calcined at 200 °C.

DOI:10.1088/1674-0068/21/04/393-400

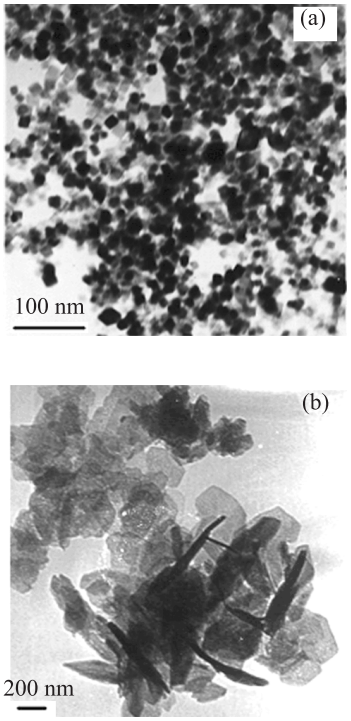

FIG. 4 TEM images of the catalysts. (a) CuO/Fe_2O_3. (b) CuO/Co_3O_4.

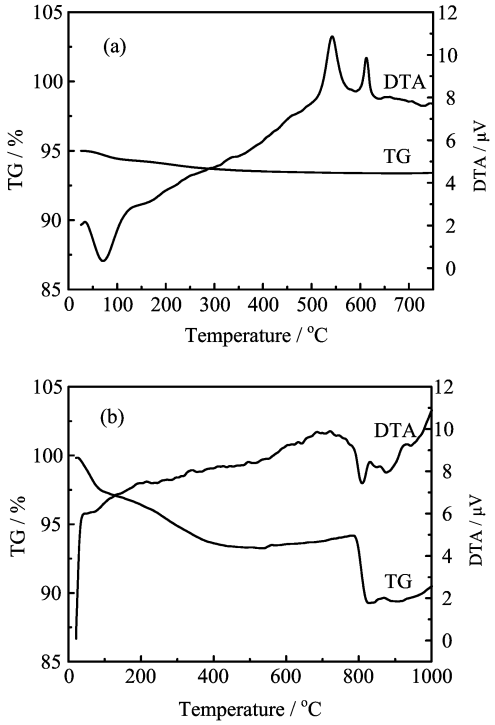

FIG. 5 TG-DTA curves of the catalysts. (a) CuO/Fe_2O_3. (b) CuO/Co_3O_4.

the corresponding temperature range. The 7% weight loss from 100 °C to 500 °C on the TG curve could result from the removal of residual hydroxyl groups and crystallization process in this region. Correspondingly, no obvious endothermic peak on the DTA curve appeared. Based on the TG-DTA results, the major phase compositions of the CuO/Fe_2O_3 are CuO/Fe_2O_3 and hydroxides. The major phase compositions of the CuO/Co_3O_4 catalysts are CuO/Co_3O_4 and hydroxides.

On the basis of the above analysis, we propose that the active phase of the catalysts is metal oxides and hydroxides. As a matter of fact, hydroxide precursors sometimes could show higher activity than the oxides as confirmed by the reports from Uphade *et al.* [40-42]. Although the CuO/Fe_2O_3 calcined at 300°C is not pure CuO and Fe_2O_3 and the CuO/Co_3O_4 calcined at 200 °C is not pure CuO and Co_3O_4, they still exhibit high catalytic activity on the reduction of NO with CO. This may be attributed to related influential factors, such as the molar ratios of the reactants, calcination temperature, active sites, particle size, the specific surface areas, and the presence of the more active hydroxides, and so forth.

B. Activity and stability tests of the catalysts

The preparation conditions of catalysts have important effects on the catalytic activity, so these effects were investigated. According to the co-precipitation as above, the molar ratios of the reactants, the volume of NaOH (2.0 mol/L) (pH value), the aging time, and the calcination temperature/time were changed while other factors were kept constant. Figure 6 shows the catalytic activity of CuO/Fe_2O_3 in different preparation conditions. From Fig.6, the optimal preparation conditions of CuO/Fe_2O_3 catalysts can be fixed as follows: molar ratios of copper to iron 1:5, pH value 9.0, ageing time 90 min, calcination temperature 300 °C and calcination time 5 h. Figure 7 shows the catalytic activity of CuO/Co_3O_4 in different preparation conditions. From Fig.7, the optimal preparation conditions of CuO/Co_3O_4 catalysts can be fixed as follows: molar ratios of copper to cobalt 1:5, volume of NaOH (2.0 mol/L) 15 mL, ageing time 5 h, calcination temperature 200 °C and calcination time 3 h.

Among these influence factors, the molar ratios of the reactants have important effect on the catalytic activity of the catalysts. The catalytic activity of CuO/Fe_2O_3 increased with increasing the molar ratios from 1:1 to 1:5 and decreased from 1:5 to 1:8. The CuO/Fe_2O_3 with molar ratio of 1:5 exhibited the highest catalytic activity with the lowest $T_{100\%}$ (80 °C) (Fig.6(a)). The $T_{100\%}$ here is defined as the temperature where the conversion of NO reaches 100%. Similarly, the catalytic activity of CuO/Co_3O_4 increased with increasing the molar ratios form 1:1 to 1:5 and decreased from 1:5 to 1:7. The CuO/Co_3O_4 catalyst with molar ratio of 1:5 exhibited high catalytic activity with lowest $T_{100\%}$ (90 °C) (Fig.7(a)). These results indicate that increas-

DOI:10.1088/1674-0068/21/04/393-400

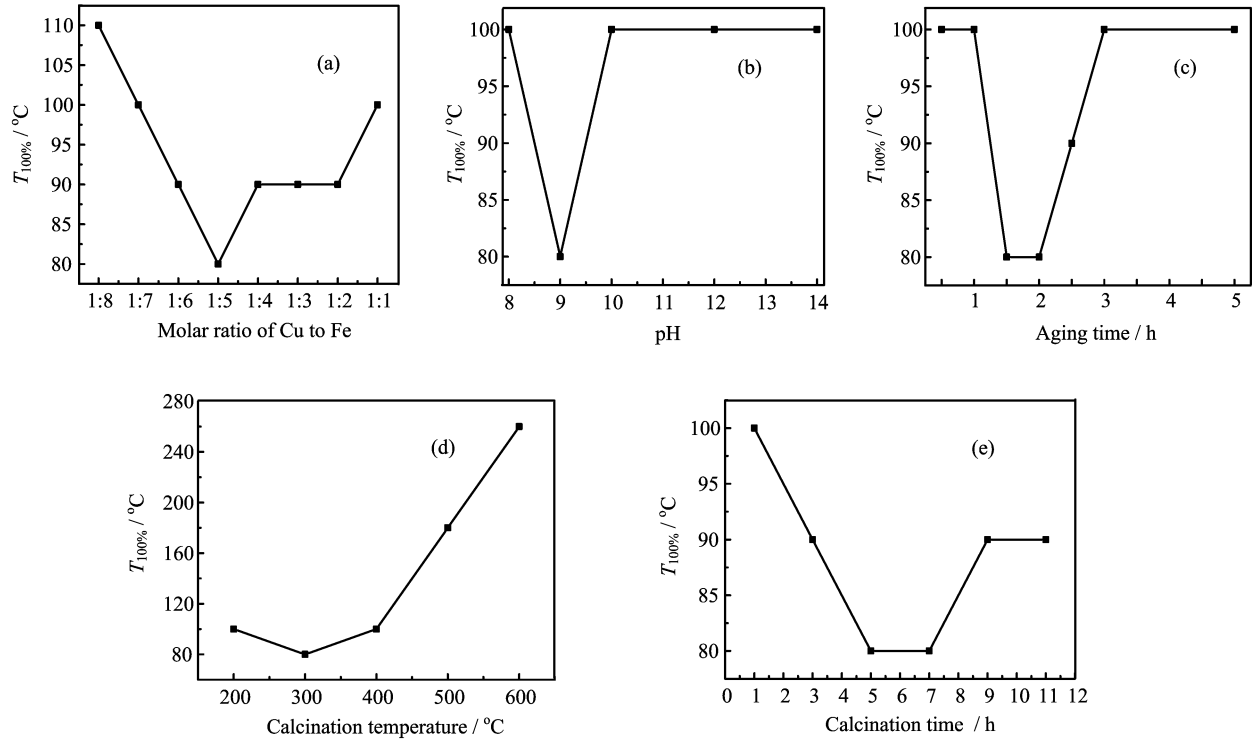

FIG. 6 The preparation conditions of the catalysts CuO/Fe_2O_3: (a) Cu:Fe, (b) pH value, (c) aging time, (d) calcination temperature, and (e) calcination time.

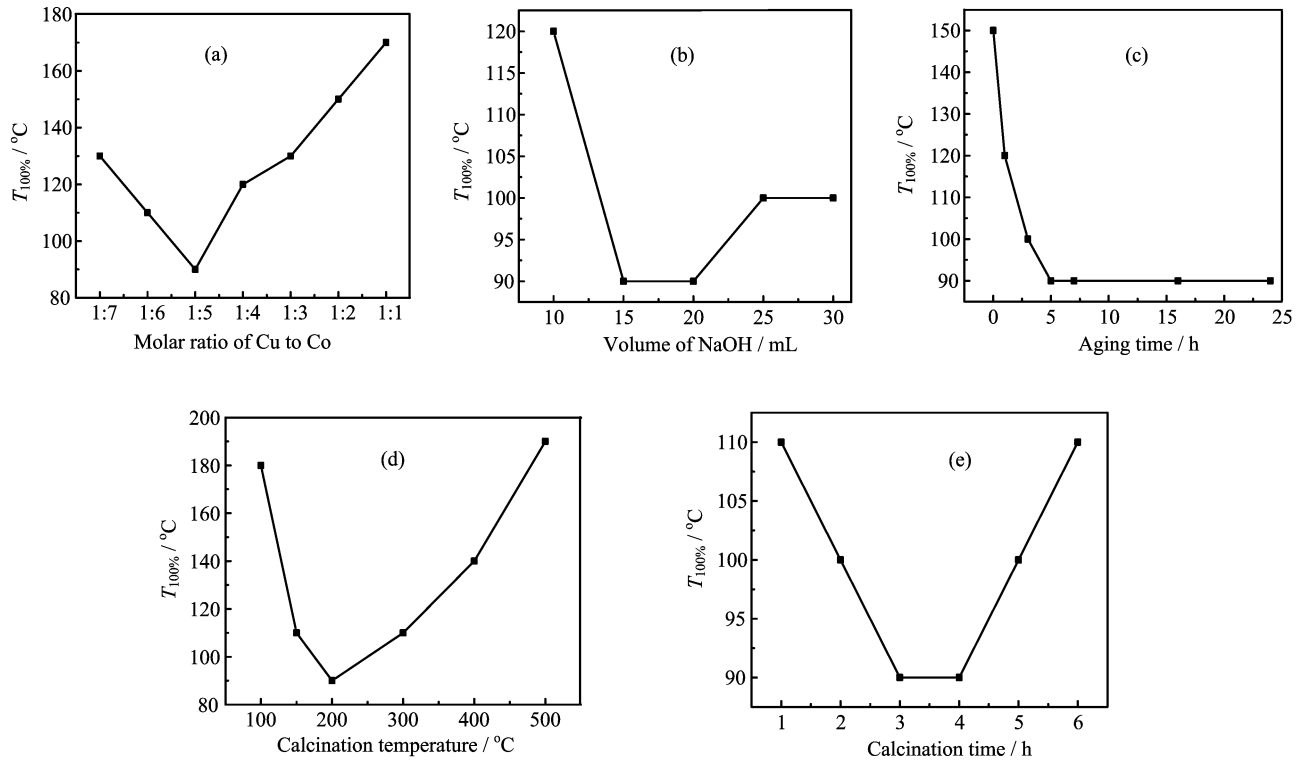

FIG. 7 The preparation conditions of the catalysts CuO/Co_3O_4: (a) Cu:Co (mol/mol), (b) NaOH solution volume, (c) aging time, (d) calcination temperature, and (e) calcination time.

DOI:10.1088/1674-0068/21/04/393-400

ing the copper content in the catalysts can promote the catalytic activity of the catalysts to some extent, but after the content of copper species achieved a certain value, the catalytic activity of the catalysts was decreased with the increasing of copper species content. These results show that the catalytic activity of the catalysts is strongly influenced by the dispersion of the copper species on the catalysts. We propose that the observed changes of the catalytic activity were probably due to the influence of different copper content in the catalysts, which results in different dispersion of copper on the catalysts and probably changes the active sites on the surface of the catalysts and the catalytically active components of the catalysts.

The calcination temperature of the catalysts also has an important effect on the catalytic activity. Figure 6(d) shows that the catalytic activity of CuO/Fe_2O_3 increased by increasing the calcination temperature from 200 °C to 300 °C and decreased sharply from 300 °C to 600 °C. The catalyst calcined at 300°C exhibited the highest catalytic activity on the reduction of NO with CO and the total conversion temperature was 80 °C. From Fig.7(d), it can be seen that the catalytic activity of CuO/Co_3O_4 increased by increasing the calcination temperature from 150 °C to 200 °C and decreased sharply from 200 °C to 500 °C. The catalyst calcined at 200 °C exhibited the highest catalytic activity on the reduction of NO with CO and the total conversion temperature was 90 °C. This may result from the catalytic activity of the catalysts. The catalytic activity of the catalysts is strongly influenced by the microstructure of the catalysts, and the structure of the catalysts is strongly influenced by the calcination temperature. The $S_{\rm BET}$ and $T_{100\%}$ of the catalysts calcined at different temperatures and the individual CuO, Fe_2O_3, Co_3O_4 catalysts are shown in Table I. In Table I, the CuO/Fe_2O_3 calcined at 300 °C exhibited the highest catalytic activity with the lowest $T_{100\%}$ and possessed the largest $S_{\rm BET}$. Correspondingly, the $S_{\rm BET}$ of the catalysts increases slowly by increasing the calcination temperature from 200 °C to 300 °C and decreases rapidly from 300 °C to 600 °C. The CuO/Co_3O_4 calcined at 200 °C exhibited the highest catalytic activity with the lowest $T_{100\%}$ and possessed the largest $S_{\rm BET}$. Correspondingly, the $S_{\rm BET}$ of the catalysts increase slowly by increasing the calcination temperature from 150 °C to 200 °C and decreases rapidly from 200 °C to 500 °C. The modification of the catalytic activity results from the modification of the catalyst $S_{\rm BET}$, which is dependent on calcination temperature. Additionally, the particle sizes of the CuO/Fe_2O_3 catalysts calcined at different temperature were obtained from the TEM images and the results are shown in Table I. From Table I, it can be seen that the particle size of the CuO/Fe_2O_3 catalysts was increased from 20 nm to 80 nm with the calcination temperature increasing from 200 °C to 600 °C, which also has a great influence on the catalytic activity of the catalysts.

TABLE I $S_{\rm BET}$ and $T_{100\%}$ of the catalysts calcined at different temperatures and the individual CuO, Fe_2O_3, Co_3O_4 catalysts.

Catalysts	Calcination Temp./°C	$S_{\rm BET}/(m^2/g)$	$T_{100\%}$	Particle size/nm
CuO	200	55.8	120	–
Co_3O_4	200	46.7	210	–
Fe_2O_3	300	58.6	150	–
CuO/Fe_2O_3	200	176.2	100	∼20
CuO/Fe_2O_3	300	256.8	80	∼20
CuO/Fe_2O_3	400	113.5	100	∼40
CuO/Fe_2O_3	500	35.6	180	∼60
CuO/Fe_2O_3	600	3.8	260	∼80
CuO/Co_3O_4	150	80.5	110	–
CuO/Co_3O_4	200	145.5	90	–
CuO/Co_3O_4	300	85.6	110	–
CuO/Co_3O_4	400	61.2	140	–
CuO/Co_3O_4	500	40.3	190	–

The catalytic activity and thermal stability of the catalysts obtained at optimal preparation conditions were investigated, and the results are presented in Fig.8. In Fig.8, the reaction temperatures were measured in the catalyst bed and were raised from 20 °C to 600 °C. It is clearly observed from Fig.8 that the catalytic activity of CuO/Fe_2O_3 and CuO/Co_3O_4 increased with the increasing of reaction temperature from 20 °C to 80 °C and from 20 °C to 90 °C. When the reaction temperature was raised from 80 °C to 600 °C for CuO/Fe_2O_3 and from 90 °C to 600 °C for CuO/Co_3O_4, the catalysts still exhibited high catalytic activity with 100% conversion of NO. To further investigate the thermal stability of the catalysts, the catalytic reaction was maintained at 600 °C for 500 min. The results showed that NO could be totally converted by the catalysts.

Thermal stability tests of the CuO/Fe_2O_3 and CuO/Co_3O_4 are shown in Fig.9, for which the reaction

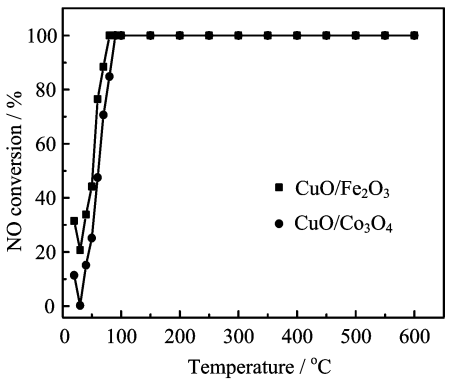

FIG. 8 Catalytic activity and theremal stabilty tests of the catalysts.

DOI:10.1088/1674-0068/21/04/393-400

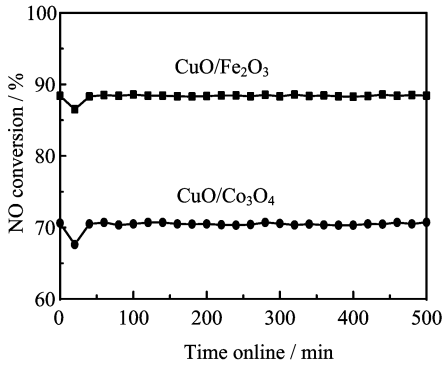

FIG. 9 Theremal stabilty tests of the catalysts.

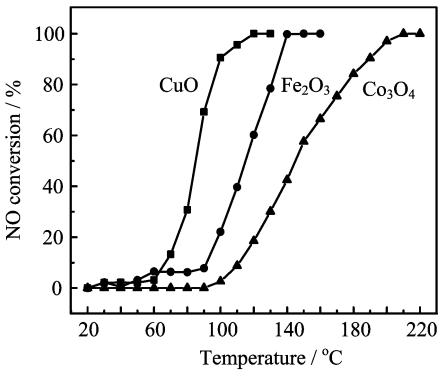

FIG. 10 Catalytic activity tests of the individual CuO, Fe_2O_3, and Co_3O_4 catalysts.

temperature was maintained at 70 °C. The catalytic activity decreased during first 20 min on line, but after this steady state period the catalytic activity was maintained over 500 min in the testing period. The decrease of catalytic activity results from the interaction between the reactants and the oxides, through which redox balance and stable surface composition were established in the initial stage. The steady state was attained after the initial stage and maintained over 500 min. The above experimental results suggest that the CuO/Fe_2O_3 and CuO/Co_3O_4 possess high catalytic activity and favorable thermal stability on NO catalytic reduction with CO in a wide temperature range and long time range.

For comparison, the individual CuO, Fe_2O_3, and Co_3O_4 catalysts were prepared through the same method as above. Their catalytic activity on the reduction of NO was evaluated in the same way and the results are shown in Fig.10. In Fig.10, the total conversion temperature of CuO, Fe_2O_3, and Co_3O_4 catalysts were 120, 150, and 210 °C, respectively. The $S_{\rm BET}$ and $T_{100\%}$ of the individual CuO, Fe_2O_3, and Co_3O_4 catalysts are presented in Table I. From Table I and Fig.10, it can be seen that the CuO/Fe_2O_3 and CuO/Co_3O_4 exhibited obviously higher catalytic activity than the individual CuO, Fe_2O_3, or Co_3O_4 catalyst, which may be ascribed to a synergistic effect of the composite oxide caused by the interfacial metal-support interaction. In the initial stage of the catalytic reduction reaction, the molecules of NO and CO were adsorbed on the surface of the catalysts, then the adsorbed molecules of NO and CO interacted over the binary mixture of the catalysts. The active intermediate compounds formed on the surface of the catalysts. Between the adsorbed molecules of NO and active intermediate compounds, a synergism interaction is possible which would result in the formation of N_2 and CO_2 [38,43-47].

IV. CONCLUSION

In this work, CuO/Fe_2O_3 and CuO/Co_3O_4 were successfully prepared by co-precipitation. The catalytic activity and thermal stability of the catalysts on the reduction of NO with CO as reducing agent were evaluated. The results indicate that the CuO/Fe_2O_3 and CuO/Co_3O_4 present obviously high catalytic activity and thermal stability on NO reduction compared to individual CuO, Fe_2O_3, or Co_3O_4 catalysts. The influence of various preparation conditions on the catalytic activity was investigated. This preparation method is simple and low cost.

[1] V. I. Parvulescu, P. Grange, and B. Delmon, Catal. Today **46**, 233 (1998).
[2] S. Bhattacharyya, and R. K. Das, Int. J. Energy. Res. **23**, 351 (1999).
[3] R. D. Zhang, A. Villanueva, H. Alamdari, and S. Kaliaguine, Appl. Catal. B **64**, 220 (2006).
[4] J. BenõÂtez, *Process Engineering and Design for Air Pollution Control*, Prentice-Hall, Englewood Cliffs, NJ. 254, (1993).
[5] H. Sjovall, L. Olsson, E. Fridell, and R. Blint, Appl. Catal. B **64**, 180 (2006).
[6] N. Apostolescu, B. Geiger, K. Hizbullah, M. T. Jan, S. Kureti, D. Reichert, F. Schott, and W. Weisweiler, Appl. Catal. B **62**, 104 (2006).
[7] F. Eigenmann, M. Maciejewski, and A. Baiker, Appl. Catal. B **62**, 311 (2006).
[8] L. Chmielarz, P. Kustrowski, A. Rafalska-Lasocha, and R. Dziembaj, Appl. Catal. B **58**, 235 (2005).
[9] A. E. Giannakas, A. K. Ladavos, and P. J. Pomonis, Appl. Catal. B **49**, 147 (2004).
[10] S. D. Peter, E. Garbowski, V. Perrichon, and M. Primet, Catal. Lett. **70**, 27 (2000).
[11] F. Garin, L. Simonot, and G. Maire, Appl. Catal. B **11**, 181 (1997).
[12] E. Joubert, X. Courtois, P. Marecot, and D. Duprez, Appl. Catal. B **64**, 103 (2006).
[13] M. Petersson, T. Holma, B. Andersson, E. Jobson, and A. Palmqvist, J. Catal. **235**, 114 (2005).
[14] K. Shimizu, and A. Satsuma, Phys. Chem. Chem. Phys. **8**, 2677 (2006).
[15] T. Grzybek, Catal. Today **119**, 125 (2007).

DOI:10.1088/1674-0068/21/04/393-400

[16] S. Mendioroz, A. B. Martin-Rojo, F. Rivera, J. C. Martin, A. Bahamonde, and M. Yates, Appl. Catal. B **64**, 161 (2006).
[17] A. P. Ferreira, C. Henriques, M. F. Ribeiro, and F. R. Ribeiro, Catal. Today **81**, 107 (2005).
[18] L. F. Cordobaa, W. M. H. Sachtlerb, and C. M. Correa, Appl. Catal. B **56**, 269 (2005).
[19] F. Lonyi, J. Valyon, L. Gutierrez, M. A. Ulla, and E. A. Lombardo, Appl. Catal. B **73**, 1 (2007).
[20] A. Pietraszek, P. D. Costa, R. Marques, P. Kornelak, T. W. Hansen, J. Camra, and M. Najbar, Catal. Today **119**, 187 (2007).
[21] A. Hornung, D. Zemlyanov, M. Muhler, and G. Ertl, Sur. Sci. **600**, 370 (2006).
[22] C. N. Costa, and A. M. Efstathiou, Appl. Catal. B **72**, 240 (2007).
[23] Y. Hasegawa, M. Haneda, Y. Kintaichi, and H. Hamada, Appl. Catal. B **60**, 41 (2005).
[24] A. A. Nikolopoulos, E. S. Stergioula, E. A. Efthimiadis, and I. A. Vasalos, Catal. Today. **54**, 439 (1999).
[25] T. V. Mironyuk, and S. N. Orlyk, Appl. Catal. B **70**, 58 (2007).
[26] Y. Okamoto, T. Kubota, and Y. Ohto, S. J. Nasu, Catal. **192**, 412 (2000).
[27] S. Bennici, and A. Gervasini, Appl. Catal. B **62**, 336 (2006).
[28] M. Iwamoto, Catal. Today **29**, 29 (1996).
[29] Y. Wan, J. X. Ma, Z. Wang, and W. Zhou, S. J. Kaliaguine, Catal. **227**, 242 (2004).
[30] S. Morfis, C. Philippopoulos, and N. Papayannakos, Appl. Clay Sci. **13**, 203 (1998).
[31] N. B. Stankova, M. S. Khristova, and D. R. Mehandjiev, J. Colloid Interface Sci. **241**, 439 (2001).
[32] X. S. Peng, H. Lin, W. F. Shangguan, and Z. Huang, Chem. Eng. Technol. **30**, 99 (2007).
[33] K. Y. Lee, K. Watanabe, and M. Misono, Appl. Catal. B **13**, 241 (1997).
[34] M. Richter, R. Eckelt, B. Parlitz, and R. Fricke, Appl. Catal. B **15**, 129 (1998).
[35] R. M. Heck, Catal. Today **53**, 519 (1999).
[36] W. E. J. Kooten, B. Liang, H. C. Krijnsen, O. L. Oudshoorn, H. P. A. Calis, and C. M. Bleek, Appl. Catal. B **21**, 203 (1999).
[37] T. Kolli, K. R. Tolonenb, U. Lassia, A. Savimakib, and R. L. Keiski, Catal. Today **100**, 297 (2005).
[38] T. N. Burdeinaya, V. A. Matyshak, V. F. Tret'yakov, L. S. Glebov, A. G. Zakirova, M. A. C. Garcia, and M. E. A. Villanueva, Appl. Catal. B **70**, 128 (2007).
[39] W. M. Shaheena and A. A. Ali, Int. J. Inorg. Mater. **3**, 1073 (2001).
[40] B. S. Uphade, Y. Yamada, T. Akita, T. Nakamura, and M. Haruta, Appl. Catal. A **215**, 137 (2001).
[41] G. J. Hutchings and M. Haruta, Appl. Catal. A **291**, 2 (2006).
[42] T. Akita, M. Okumura, K. Tanaka, M. Kohyama, and M. Haruta, Catal. Today **117**, 62 (2006).
[43] R. Burch, and A. R. J. Flambard, Catal. **78**, 389 (1982).
[44] T. N. Burdeinaya, V. A. Matyshak, V. F. Tret'yakov, O. S Mokrushin, and L. S. Glebov, Kinet. Katal. **41**, 377 (2000).
[45] C. Yokoyama and M. Misono, Catal. Lett. **29**, 1 (1994).
[46] K. A. Bethke and H. H. Kung, J. Catal. **172**, 93 (1997).
[47] J. C. Yan, H. H. Kung, W. M. H. Sachtler, and M. C. Kung, J. Catal. **175**, 294 (1998).

DOI:10.1088/1674-0068/21/04/393-400